Full Length Article

JHS(E)

Journal of Hand Surgery
(European Volume)
0(0) 1–7

DOI: 10.1177/1753193420943400
journals.sagepub.com/home/jhs

Effects of axial load on in vivo scaphoid and lunate kinematics using four-dimensional computed tomography

Michelle Brinkhorst[1], Geert Streekstra[2,3], Joost van Rosmalen[4], Simon Strackee[5] and Steven Hovius[6,7]

Abstract

This in vivo study investigated the effect of axial load on lunate and scaphoid kinematics during flexion–extension and radial–ulnar deviation of the uninjured wrist using four-dimensional computed tomography. We found that applying axial load to the wrist results in a more flexed, radially deviated and pronated position of the lunate and scaphoid during flexion–extension of the wrist compared with when no load is applied. A larger pronation and supination range of the lunate and scaphoid was seen when the wrist was flexed and extended under axial load, whereas a larger flexion and extension range of the lunate and scaphoid occurred during radial–ulnar deviation of the wrist when axial load was applied.

Keywords

Wrist joint, in-vivo kinematics, carpal kinematics, dynamic, four-dimensional CT imaging

Date received: 30th April 2020; revised: 23rd June 2020; accepted: 28th June 2020

Introduction

The lunate and scaphoid form a complex joint that has been studied extensively. Together with the triquetrum, they form an intercalated segment between the distal carpal row and the bones of the forearm. The alignment of the bones is maintained through the shape of the bones, surrounding joint surfaces, ligaments and the axial load crossing the joint from the metacarpals to the forearm muscles. In 1997, Kobayahi et al. (1997b) described how when axial load is applied, the wrist maintains its stability; flexion, radial deviation and supination of the proximal row is facilitated as a result of a complex mechanism, which involved interaction between the intercarpal and midcarpal joint geometries and different ligament constrains.

Instability of the scapholunate joint is most commonly caused by injury to the scapholunate interosseous ligament (Kitay and Wolfe, 2012). If left untreated, this injury will lead to advanced secondary osteoarthritis, such as scapholunate advanced collapse (SLAC) (O'Meeghan et al., 2003). Early diagnosis is therefore crucial to enable early treatment, which may prevent persistent and usually progressive instability resulting in degenerative osteoarthritis. In this context, it is important to understand carpal kinematics in the uninjured wrist before interpreting the carpal kinematics of the injured wrist and making subsequent treatment decisions.

Diagnostic techniques have evolved over the past decades. Specific radiographs, such as the clenched fist view, cineradiography, computerized tomography (CT) and magnetic resonance imaging (MRI) provided an initial understanding of wrist kinematics.

[1]Department of Plastic, Reconstructive and Hand Surgery, University Medical Center Rotterdam, Rotterdam, The Netherlands
[2]Department of Biomedical Engineering and Physics, Amsterdam UMC, University of Amsterdam, The Netherlands
[3]Department of Radiology, Amsterdam UMC, University of Amsterdam, The Netherlands
[4]Department of Biostatistics, University Medical Center Rotterdam, Rotterdam, The Netherlands
[5]Department of Plastic, Reconstructive and Hand Surgery, Amsterdam UMC, University of Amsterdam, The Netherlands
[6]Xpert Clinic, Hand and Wrist Clinic, Nijmegen, The Netherlands
[7]Department of Plastic, Reconstructive and Hand Surgery, Radboudumc, Nijmegen, The Netherlands

Corresponding Author:
Michelle Brinkhorst, PO Box 2040, Room Na-2206, 3000 CA Rotterdam, The Netherlands.
Email: m.brinkhorst@erasmusmc.nl

More recently, dynamic four-dimensional CT (4-D CT) studies have been introduced (Athlani et al., 2020; Carr et al., 2019; de Roo et al., 2019; Rauch et al., 2018; White et al., 2019). Current studies using 4-D CT have focused on the gap size between the scaphoid and lunate when axial load is applied or on carpal kinematics during the dart-throwing motion (Demehri et al., 2016; Edirisinghe et al., 2014; Garcia-Elias et al., 2014; Kelly et al., 2018). The application of tendon loading during cadaveric experiments to simulate natural stabilizing joint compression has shown changes in the orientation of the carpal bones and carpal kinematics (Foumani et al., 2010; Gupta, 2002; Kobayashi et al., 1997b). The effects of axial load on scaphoid and lunate kinematics during active flexion–extension and radial–ulnar deviation are yet unknown, but thought to be of great importance in diagnosing and treating carpal and ligamentous injury. The aim of this in vivo study was to investigate the effect of axial load on lunate and scaphoid kinematics during flexion–extension and radial–ulnar deviation of the uninjured wrist using 4-D CT.

Methods

Ethical approval was obtained from our institution before the study. Written informed consent was obtained from all participants. Both wrists of 20 uninjured participants (11 men and nine women) with a mean age of 27 years (SD 4; range 21–40) were studied. All participants stated they had not had any wrist surgery, significant trauma to their wrists or any symptoms of carpal instability. The Beighton score was used to assess hypermobility with a score of 4 being the clinical level for hypermobility (Beighton et al., 1973). All participants were Caucasian and their individual Beighton scores were all less than 4, so no participants were excluded and all 40 wrists were used in the analysis.

Participants were put in a prone position with one arm 180° abducted; the forearm was placed in a custom-made motion guiding device (de Roo et al., 2019) with the elbow extended and the forearm in pronation fixed to a framework to guide the hand and wrist during the 4-D CT recordings. Metacarpals were placed in a natural position on a handle that was attached to the framework. The handle was designed to measure grip strength, which could be assessed by the participant and the study investigator during CT recordings. Load on the metacarpals is directed along the longitudinal axis of the bone. By clenching the wrist, the force applied on the metacarpals compressed the wrist. Participants were instructed to lightly grab the handlebar when no axial load was applied, or to clench their fist to produce 100 N (approximately 10 kg). Each participant received individualized information and training before scanning to ensure they understood the flexion–extension and radial–ulnar deviation motion of the wrist and the speed needed to complete each motion cycle.

A Brilliance 64-slice CT scanner (Philips Medical System, Best, The Netherlands) was used. A static CT image (120 kV, 75 mAs) of the wrist in neutral was taken to reconstruct the bony geometry of the scaphoid, lunate, capitate and distal portion of the radius (the length scanned was 4 cm). The neutral position of the wrist was defined as the dorsal part of the middle metacarpal being aligned with the dorsal part of the radius. Subsequently, one flexion–extension followed by a radial–ulnar deviation motion movement was imaged with a 4-D CT protocol (120 kV, 15 mAs, 64×0.625 mm). Participants started each motion cycle with a relaxed grip around the handlebar. After completion of one motion cycle, a pause of 4 minutes was taken and subsequently the same motion cycle was repeated with a clenched fist. In all, four scans per wrist were obtained. Each scan was made as a smooth motion within 10 seconds.

After completion of all four dynamic scans of both wrists, the scaphoid, lunate, capitate and distal portion of the radius were segmented in the static scan using a region-growing algorithm described by Carelsen and Foumani (Foumani et al., 2009). All scans of the left wrist were mirrored to present as a right wrist to assist data analysis. Using custom-made software, an estimation of the rotational parameters of each individual bone relative to the neutral position was obtained by registering the segmented bones from the neutral scan to the corresponding bones of each timeframe of the 4-D CT scan. Carpal bone kinematical parameters, during wrist motion, were calculated for each time frame of the 4-D CT (Woltring, 1994). Dobbe et al. (2019) showed this method of 4-D CT data analysis to be accurate and precise with positioning errors <0.23 mm and $<0.78°$. Motion patterns of the scaphoid, lunate and capitate were studied using an anatomically based radial coordinate system, described by Kobayashi et al. (1997a). Essentially, the axes of the scaphoid, lunate and capitate were defined as being parallel to this anatomical coordinate system of the radius with the wrist in a neutral position. Global wrist motion was described as the rotation in degrees of the capitate relative to the radius (de Lange et al., 1985; Neu et al., 2001). Carpal motion was quantified as rotation in degrees of the scaphoid, lunate and capitate relative to the radius. Flexion (X+), extension (X−), radial deviation (Y+), ulnar deviation (Y−), supination (Z+)

and pronation (Z−) were defined as the rotation in degrees around the axes of the anatomical coordinate system of the radius (de Roo et al., 2019; Foumani et al., 2009; Kobayashi et al., 1997a).

Linear mixed models were used to compare the carpal motion patterns with and without axial load (Verbeke and Molenberghs, 2001). The different values of global wrist motion were considered as repeated measurements. To account for correlations between observations within a motion cycle, observations of different levels of global wrist motion were assumed to be correlated according to a first-order autoregressive moving average (ARMA(1,1)) covariance structure. The effect of this covariance structure is that higher correlations are assumed between similar levels of global wrist motion than between global wrist motions that are far apart. To further account for the within-subject correlations, random intercepts and random slopes of global wrist motion were included in the model, so that the level of the carpal motion pattern and its linear association with global wrist motion were assumed to vary among the participants. The selection of the error covariance structure and the random effects structure was based on information criteria that take into account the goodness of fit and the complexity of different possible model specifications. To simplify the estimation of the model, only the observations were included per 5° of global wrist motion. Independent variables in the model were global wrist motion, axial load and the interaction effect of load and global wrist motion. All models were stratified by rotational axis (flexion–extension, radial–ulnar deviation and pronation–supination) and carpal bone (scaphoid or lunate). All statistical tests were two-sided and a significance level of 5% was set.

Results

Carpal kinematics during flexion–extension of the wrist (Table 1; Figure 1)

During flexion and extension of the wrist, the lunate and scaphoid closely follow the motion of the capitate. Without axial loading, the lunate showed less flexion–extension than the scaphoid (46° vs 75°). When axial load was applied, the scaphoid and lunate had a significantly more flexed position (estimated effect approximately 4° for both) compared with no axial loading. This more flexed position during axial load had no influence on flexion–extension range of the lunate or scaphoid (respectively, 44° and 75°).

In the loaded and unloaded situations, the lunate and scaphoid showed similar radial–ulnar deviation motion patterns during flexion–extension of the wrist (difference of estimated interaction effect of axial load was <0.01°). When the wrist was extended they deviated radially and when the wrist was flexed they deviated ulnarly. Without axial loading, the lunate and scaphoid showed similar ranges of radial–ulnar deviation (respectively, 11° and 13°) during flexion–extension of the wrist. When axial loading was applied, the lunate had a small but significantly more radially deviated position. This more radially deviated position under axial load had no influence on the radial–ulnar deviation range (10°) of the lunate.

The pronation–supination pattern of the lunate and scaphoid during flexion–extension of the wrist was similar and small. When the wrist was extended they supinated and when the wrist was flexed they pronated. Without axial loading, the range of motion was relatively small (respectively, 7° and 13°). When axial loading was applied, the lunate and scaphoid showed a small but significantly more pronated position than when no load was applied. Also, a significantly smaller range of pronation and supination of the lunate and scaphoid was seen (respectively, 4° and 12°).

Carpal kinematics during radial–ulnar deviation of the wrist (Table 1; Figure 2)

During radial–ulnar deviation of the wrist the lunate and scaphoid showed similar motion patterns. When the wrist was ulnarly deviated the lunate and scaphoid extended and when the wrist was radially deviated they flexed. Without axial loading, the lunate showed slightly more flexion–extension than the scaphoid (respectively, 29° vs 24°). When axial load was applied, the lunate and scaphoid did not show any change in their position with no axial loading. Although no change in position was found, the lunate and scaphoid showed a significantly larger flexion–extension range (respectively, 32° and 26°) than the range without loading.

The lunate and scaphoid showed similar radial–ulnar deviation motion patterns with and without axial load during radial–ulnar deviation of the wrist. No changes in radial–ulnar deviation range or position were observed when axial loading was compared with no axial loading. With and without axial loading, almost no pronation–supination of the lunate and scaphoid during radial–ulnar deviation of the wrist was seen (1° for both).

Discussion

The aim of this in vivo study was to assess the effect of axial load on lunate and scaphoid kinematics

Table 1. Estimated effects of global wrist motion and load in a linear mixed model.

	Flexion–extension wrist		Radial–ulnar deviation wrist	
	Difference (95% CI) (°)	*p*-value	Difference (95% CI) (°)	*p*-value
	Estimated effect of axial load			
Lunate				
FE	−3.9 (−5.7 to −2.1)	<**0.001**	−0.6 (−2.0 to 0.8)	0.38
RU	−1.6 (−3.1 to −0.1)	**0.035**	−0.8 (−1.7 to 0.1)	0.10
Pro–sup	0.7 (0.1 to 1.4)	**0.033**	0.6 (0.0 to 1.2)	0.05
Scaphoid				
FE	−3.8 (−5.4 to −2.2)	<**0.001**	−1.1 (−3.0 to 0.8)	0.27
RU	−1.4 (−3.7 to −0.9)	0.23	−0.7 (−1,6 to 0.2)	0.12
Pro–sup	1.2 (0.4 to 2.1)	**0.003**	0.7 (−0.0 to 1.5)	0.06
Capitate				
FE	—	—	0.5 (−1.20 to 2.3)	0.54
RU	−4.4 (−6.9 to −1.9)	<**0.001**	—	—
Pro–sup	0.0 (−1.3 to 1.3)	0.98	1.7 (0.9 to 2.5)	<**0.001**
	Estimated interaction effect of axial load and wrist motion			
Lunate				
FE	−0.004 (−0.03 to −0.02)	0.73	−0.08 (−0.11 to −0.04)	<**0.001**
RU	0.005 (−0.01 to −0.02)	0.43	0.02 (−0.007 to -0.04)	0.19
Pro–sup	−0.02 (−0.03 to −0.01)	<**0.001**	−0.01 (−0.03 to 0.002)	0.08
Scaphoid				
FE	−0.008 (−0.03 to 0.01)	0.42	−0.06 (−0.10 to -0.02)	**0.007**
RU	0.009 (−0.01 to −0.02)	0.24	−0,02 (−0.04 to 0.008)	0.18
Pro–sup	−0.01 (−0.02 to −0.003)	**0.006**	−0.02 (−0.04 to −0.003)	**0.02**
Capitate				
FE	—	—	−0.02 (−0.05 to 0.02)	0.40
RU	−0.02 (−0.04 to −0.002)	**0.03**	—	—
Pro–sup	−0.016 (−0.03 to −0.002)	**0.02**	−0.04 (−0.06 to −0.02)	<**0.001**

To determine the combined effect of axial load (yes/no) and wrist motion (in degrees), the main effects and the interaction effects of these variables were used as fixed effects in a linear mixed model. The main effect of load describes the effect of load on rotation/position of the carpal bone at a global wrist motion of 0°; the interaction effect describes the increase in the effect of load on rotation per degree increase in wrist motion, which describes the motion pattern of the carpal bone.
FE: flexion–extension motion; RU: radial–ulnar deviation motion; Pro–sup: pronation–supination motion; CI: confidence interval.
Statistically significant values are shown in bold font.

during flexion–extension and radial–ulnar deviation in the uninjured wrist using 4-D CT. We found that the application of axial load to the wrist results in a more flexed, radially deviated and pronated position of the lunate and scaphoid during flexion–extension of the wrist compared with when there is no load. This phenomenon was not seen when axial load was applied during radial–ulnar deviation of the wrist. A larger pronation and supination range of the lunate and scaphoid during axial load was seen when the wrist was flexed and extended. A larger flexion and extension range of the lunate and scaphoid was seen during radial–ulnar deviation of the wrist when axial load was applied.

The diagnosis of scapholunate injuries can be difficult. Injuries of the scapholunate ligament can vary in severity from partial disruption to a complete tear. Several imaging options are available for diagnosis, all with their own flaws. Plain radiographs and MRI scans lack specificity as they are static examinations, which cannot detect alterations in carpal motion (Bateni et al., 2013). Stress radiography, like the clenched pencil view, have low sensitivity and specificity regarding ligament injuries (Kuo and Wolfe, 2008). Dynamic imaging techniques, such as cineradiography, have high sensitivity and specificity, but may miss subtle bony changes and diagnosis can be investigator dependent as there is a steep learning curve (Pliefke et al., 2008; Sulkers et al., 2018). Wrist arthroscopy remains the reference standard owing to its ability to assess the kinematic behaviour of the carpal bones. However, it is an invasive method

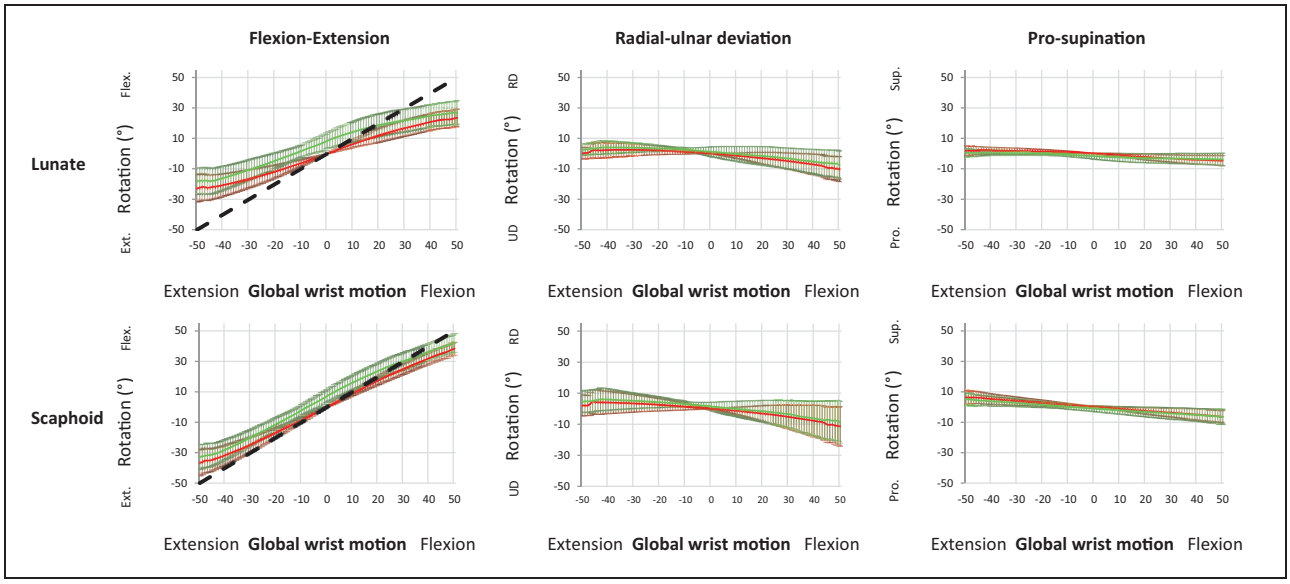

Figure 1. Comparison of loaded (green) and non-loaded (red) motion patterns in healthy volunteers during flexion–extension of the wrist. Mean and standard deviations of flexion–extension, radial–ulnar deviation and pronation–supination of the lunate and scaphoid are plotted for every degree of wrist motion. Flexion–extension motion of the capitate is presented as a straight dotted line, as the flexion–extension motion of the capitate was used to define the global wrist motion.
Ext.: extension; Flex.: flexion; UD: ulnar deviation; RD: radial deviation; Pro.: pronation; Sup.: supination.

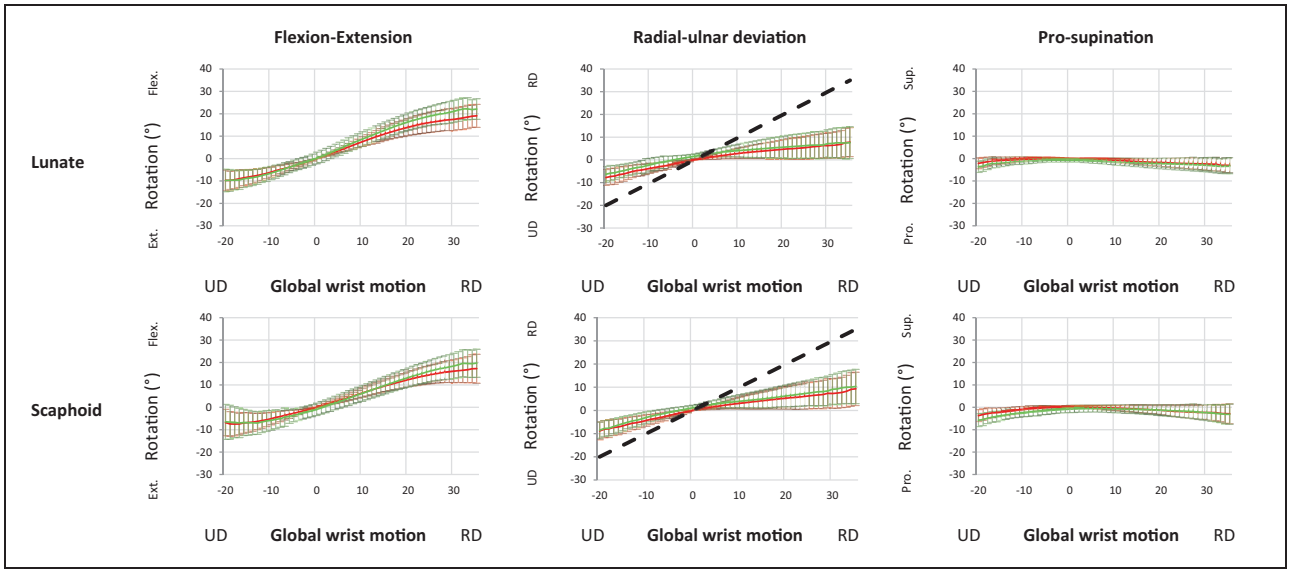

Figure 2. Comparison of loaded (green) and non-loaded (red) motion patterns in healthy volunteers during radial–ulnar deviation of the wrist. Mean and standard deviations of flexion–extension, radial–ulnar deviation and pronation–supination of the lunate and scaphoid are plotted for every degree of wrist motion. Flexion–extension motion of the capitate is presented as a straight dotted line, as the radial–ulnar deviation motion of the capitate was used to define the global wrist motion.
Ext.: extension; Flex.: flexion; UD: ulnar deviation; RD: radial deviation; Pro.: pronation; Sup.: supination.

with some risks, for example nerve injury, infection and stiffness. Furthermore, traction on the wrist is not physiological nor is the insertion of a 2.7-mm wide instrument. The introduction of 4-D CT could provide a non-invasive alternative to assess carpal kinematics and may help to diagnose acute stage scapholunate ligament injuries, without the disadvantages of other methods.

Axial load has been used to identify dynamic instability patterns by precipitating subtle carpal malalignment through clenched fist radiographs (Lee et al., 2011; Truong et al., 1994). It is, however, highly dependent of the position of the wrist during compression. Few dynamic studies of the wrist have been done with the joint loaded (Foumani et al., 2010; Meade et al., 1990; Truong et al., 1994; Wolfe et al., 1997). An altered motion pattern during axial load compression may be an indicator of scapholunate ligament injury. However, an understanding of normal imaging anatomy is necessary before defining pathology.

Kobayashi et al. (1997b) studied the changes in carpal bone alignment in 13 cadaver specimens secondary to axial load. A load of 89 N was applied through the wrist motor tendons followed by biplanar radiographic analysis of the carpal bones with the wrist in a neutral position. They concluded that with axial loading the scaphoid and lunate rotated into a more flexed, radially deviated and supinated position. Owing to the oblique alignment of the scaphoid in the sagittal and coronal planes, axial load will result in a flexed and radially deviated position of the scaphoid. The present study found similar results when axial load was applied during flexion–extension of the wrist. However, these changes were not seen when the wrist was radial–ulnar deviated. These differences may be because load in the wrist is not evenly distributed and may be localized to specific areas during specific wrist movements (Short et al., 1997).

Gupta (2002) studied the effect of physiological axial loading on carpal alignment in lateral radiographs of 20 uninjured wrists before and after general anaesthesia with muscle relaxants. It was found that physiological axial load, applied by the forearm muscles, tends to flex the lunate and scaphoid. It was suggested that the scaphoid is subject to more force than other bones of the proximal carpal row. Force through the trapezium and trapezoid, and the anteriorly placed distal pole of the scaphoid, cause it to be pushed into a flexed position when axial load is applied. The lunate is subsequently forced into flexion because of the attachment of the scapholunate ligament. In the present study we also found a more flexed position of the lunate and scaphoid when axial loading was applied during flexion–extension of the wrist.

Foumani et al. (2010) studied the effect of tendon loading on in-vitro carpal kinematics using a four-dimensional rotational X-ray imaging system. Carpal kinematics were compared with and without applying 50 N load to the extensor tendons and 50 N load to the flexor tendons while the wrist was passively moved into flexion–extension or radial–ulnar deviation. In contrast to the results in our study and previous studies investigating the effects of load on carpal kinematics (Gupta, 2002; Kobayashi et al., 1997b), they found that during flexion–extension of the wrist the scaphoid and lunate were less flexed when load was applied. They also observed that during radial–ulnar deviation of the wrist, the lunate and scaphoid were more radially deviated and showed more supination. The data in our study did not support this. This may be a result of different experimental conditions; their study was a cadaver study and the wrist moved passively by a motion device.

There are several limitations to our study. The sample was relatively small. However, it is currently the largest group of in vivo uninjured wrists that has been studied with the dynamic 4-D CT method. It was assumed after the selection process that all wrists were uninjured and 'normal'. Nevertheless, this does not rule out wrist disorders or congenitally different shapes of the carpal bones affecting the findings. Implementation of this technique in clinical practice will require training of medical staff on how to position and instruct the patient and how to analyse the data. Radiation exposure should always be kept to a minimum. However, the maximum effective dose in our study was approximately 0.15 mSv for each participant. This is classified as having minor risk, according to the International Commission on Radiological Protection (ICRP) (ICoRP, 1991).

The data in this study provide a better understanding of in vivo carpal kinematics in uninjured wrists and show the effect of axial loading on the lunate and scaphoid kinematics. They may serve as normative data for future studies focusing on carpal kinematics after ligament repair, scaphoid fractures or in the diagnosis of ligamentous injury.

Acknowledgements The authors wish to thank Wim Scheurs and Niels Kind for designing and building the motion guiding device, Mahyar Fouhmani for his technical help and Ruud Selles for his general support.

Declaration of conflicting interests The authors declare no potential conflicts of interest with respect to the research, authorship, and/or publication of this article.

Funding statement The authors disclosed receipt of the following financial support for the research, authorship, and/or publication of this article: this work was supported by a fund from Fonds NutsOhra [1301-030].

Ethical approval This study was approved by the Medical Ethical Committee of the Amsterdam University Medical Centers location AMC in Amsterdam (NL44780.018.13 2013_242).

Informed consent Written informed consent was obtained from all subjects before the study.

References

Athlani L, Rouizi K, Granero J et al. Assessment of scapholunate instability with dynamic computed tomography. J Hand Surg Eur. 2020, 45: 375–82.

Bateni CP, Bartolotta RJ, Richardson ML, Mulcahy H, Allan CH. Imaging key wrist ligaments: what the surgeon needs the radiologist to know. Am J Roentgenol. 2013, 200: 1089–95.

Beighton P, Solomon L, Soskolne CL. Articular mobility in an African population. Ann Rheum Dis. 1973, 32: 413–8.

Carr R, MacLean S, Slavotinek J, Bain GI. Four-dimensional computed tomography scanning for dynamic wrist disorders: prospective analysis and recommendations for clinical utility. J Wrist Surg. 2019, 8: 161–7.

Dobbe JGG, de Roo MGA, Visschers JC, Strackee SD, Streekstra GJ. Evaluation of a quantitative method for carpal motion analysis using clinical 3-D and 4-D CT protocols. IEEE Trans Med Imaging. 2019, 4: 1048–57.

de Lange A, Kauer JM, Huiskes R. Kinematic behavior of the human wrist joint: a roentgen-stereophotogrammetric analysis. J Orthop Res. 1985, 3: 56–64.

de Roo MGA, Muurling M, Dobbe JGG, Brinkhorst ME, Streekstra GJ, Strackee SD. A four-dimensional-CT study of in vivo scapholunate rotation axes: possible implications for scapholunate ligament reconstruction. J Hand Surg Eur. 2019, 44: 479–87.

Demehri S, Hafezi-Nejad N, Morelli JN et al. Scapholunate kinematics of asymptomatic wrists in comparison with symptomatic contralateral wrists using four-dimensional CT examinations: initial clinical experience. Skeletal Radiol. 2016, 45: 437–46.

Edirisinghe Y, Troupis JM, Patel M, Smith J, Crossett M. Dynamic motion analysis of dart throwers motion visualized through computerized tomography and calculation of the axis of rotation. J Hand Surg Eur. 2014, 39: 364–72.

Foumani M, Blankevoort L, Stekelenburg C et al. The effect of tendon loading on in-vitro carpal kinematics of the wrist joint. J Biomech. 2010, 43: 1799–805.

Foumani M, Strackee SD, Jonges R et al. In-vivo three-dimensional carpal bone kinematics during flexion-extension and radio-ulnar deviation of the wrist: dynamic motion versus step-wise static wrist positions. J Biomech. 2009, 42: 2664–71.

Garcia-Elias M, Alomar Serrallach X, Monill Serra J. Dart-throwing motion in patients with scapholunate instability: a dynamic four-dimensional computed tomography study. J Hand Surg Eur. 2014, 39: 346–52.

Gupta A. Change of carpal alignment under anaesthesia: role of physiological axial loading on carpus. Clin Biomech (Bristol, Avon). 2002, 17: 660–5.

ICoRP I. Radiological protection in biomedical research. A report of committee 3 adopted by the International Commission on Radiological Protection. Ann ICRP. 1991, 22: 1–28, v–xxiv.

Kelly PM, Hopkins JG, Furey AJ, Squire DS. Dynamic CT scan of the normal scapholunate joint in a clenched fist and radial and ulnar deviation. Hand (NY). 2018, 13: 666–70. DOI: 10.1177/1558944717726372.

Kitay A, Wolfe SW. Scapholunate instability: current concepts in diagnosis and management. J Hand Surg Am. 2012, 37: 2175–96.

Kobayashi M, Berger RA, Nagy L et al. Normal kinematics of carpal bones: a three-dimensional analysis of carpal bone motion relative to the radius. J Biomech. 1997a, 30: 787–93.

Kobayashi M, Garcia-Elias M, Nagy L et al. Axial loading induces rotation of the proximal carpal row bones around unique screw-displacement axes. J Biomech. 1997b, 30: 1165–7.

Kuo CE, Wolfe SW. Scapholunate instability: current concepts in diagnosis and management. J Hand Surg Am. 2008, 33: 998–1013.

Lee SK, Desai H, Silver B, Dhaliwal G, Paksima N. Comparison of radiographic stress views for scapholunate dynamic instability in a cadaver model. J Hand Surg Am. 2011, 36: 1149–57.

Meade TD, Schneider LH, Cherry K. Radiographic analysis of selective ligament sectioning at the carpal scaphoid: a cadaver study. J Hand Surg Am. 1990, 15: 855–62.

Neu CP, Crisco JJ, Wolfe SW. In vivo kinematic behavior of the radio-capitate joint during wrist flexion-extension and radio-ulnar deviation. J Biomech. 2001, 34: 1429–38.

O'Meeghan CJ, Stuart W, Mamo V, Stanley JK, Trail IA. The natural history of an untreated isolated scapholunate interosseus ligament injury. J Hand Surg Br. 2003, 28: 307–10.

Pliefke J, Stengel D, Rademacher G, Mutze S, Ekkernkamp A, Eisenschenk A. Diagnostic accuracy of plain radiographs and cineradiography in diagnosing traumatic scapholunate dissociation. Skeletal Radiol. 2008, 37: 139–45.

Rauch A, Arab WA, Dap F, Dautel G, Blum A, Gondim Teixeira PA. Four-dimensional CT analysis of wrist kinematics during radio-ulnar deviation. Radiology. 2018, 289: 750–8.

Short WH, Werner FW, Fortino MD, Mann KA. Analysis of the kinematics of the scaphoid and lunate in the intact wrist joint. Hand Clin. 1997, 13: 93–108.

Sulkers GSI, Strackee SD, Schep NWL, Maas M. Wrist cineradiography: a protocol for diagnosing carpal instability. J Hand Surg Eur. 2018, 43: 174–8.

Truong NP, Mann FA, Gilula LA, Kang SW. Wrist instability series: increased yield with clinical-radiologic screening criteria. Radiology. 1994, 192: 481–4.

Verbeke G, Molenberghs G. *Linear mixed models for longitudinal data*. Springer: New York, 2001.

White J, Couzens G, Jeffery C. The use of 4D-CT in assessing wrist kinematics and pathology: a narrative view. Bone Joint J Br. 2019, 101: 1325–30.

Wolfe SW, Gupta A, Crisco JJ 3rd. Kinematics of the scaphoid shift test. J Hand Surg Am. 1997, 22: 801–6.

Woltring HJ. 3-D attitude representation of human joints: a standardization proposal. J Biomech. 1994, 27: 1399–414.